Water, Dust, and Environmental Justice: The Case of Agricultural Water Diversions*

Ryan Abman[1], Eric C. Edwards[2], and Danae Hernandez-Cortes[3]

[1]San Diego State University
[2]University of California Davis
[3]Arizona State University

December 2023

Abstract

Water diversions for agriculture reduce ecosystem services provided by saline lakes around the world. Exposed lakebed surfaces are major sources of dust emissions that may exacerbate existing environmental inequities. This paper studies the effects of water diversions and their impacts on particulate pollution arising from reduced inflows to the Salton Sea via a spatially-explicit particle transport model and changing lakebed exposure. We demonstrate that lakebed dust emissions increased ambient PM_{10} and $PM_{2.5}$ concentrations and worsened environmental inequalities, with historically disadvantaged communities receiving a disproportionate increase in pollution. Water diversion decisions are often determined by political processes, and our findings demonstrate the need for analysis of distributional impacts to ensure equitable compensation.

*We thank participants of the AAEA Conference on Economics of Inequity in Agricultural, Food, and Environmental Systems, University of New Mexico Economics Department seminar, and OSWEEET for helpful comments. This project was partially funded by the USDA National Institute of Food and Agriculture (Hatch project 1017720 and multi-state project 1020662).

1 Introduction

In situ water in streams, rivers, and lakes provides a suite of valuable ecosystem services including transportation, habitat, electricity production, and nutrient and waste removal. Consumptive water use (e.g. irrigation) and the diversion of water out of basin reduce these services. Food production via irrigated agriculture accounts for the largest share of freshwater consumption, exceeding 85% of consumptive use worldwide (D'Odorico et al., 2020). While agricultural water diversions decrease the volume available for ecosystems, there is limited understanding of the distribution of these losses across disadvantaged populations

The effect of agriculture on ecosystem services via its use of water is illustrated clearly in the world's saline lakes where increased consumptive water use and changing patterns of water diversions have created an environmental and health crisis (Wurtsbaugh et al., 2017). When water inflows to lakes like the Great Salt Lake and the Aral Sea decrease, ecosystem services are reduced. The most costly effect is the increased dust emissions from the exposed lakebed surface, referred to as playa (Wurtsbaugh et al., 2017). Playa sediments are important local and regional sources of dust and account for up to a third of global dust emissions (Van Pelt et al., 2020; Dickey et al., 2023; Jones, 2020). Dust is a key pollutant that has been associated with infant mortality, asthma, and cardiovascular and respiratory morbidity and mortality (Heft-Neal et al., 2020; Kittle, 2000a). Because reduced inflows increase dust pollution exposure in surrounding communities, open questions exist about whether playa dust exacerbates existing environmental inequalities by disproportionately affecting historically disadvantaged communities (Johnston et al., 2019).

In this paper, we provide a novel method for linking playa exposure to increased air pollution via a particle transport model. Playa are some of the most emissive land surfaces in the world, with emissivity defined as the potential of a surface to release fine particulates into the atmosphere when subjected to shear stress via wind (Dickey et al., 2023). Our approach allows us to estimate the effects of saline lake decline on spatially-explicit changes in air pollution and to estimate the distribution of these impacts on at-risk and disadvantaged populations. We apply our method to the case of the Salton Sea in California to examine the spatial distribution on dust pollution as a result of changes in playa exposure.

The Salton Sea offers a unique setting to study this question due to contemporary changes in

policies and playa exposure centering around the transfer of water from the Imperial Irrigation District to San Diego County. As a result of the transfer program, dust-related air pollutants such as PM_{10} and $PM_{2.5}$ increased, especially after key changes in the methods and amount of transfer starting in 2012 (Ge et al., 2023). Other studies have also found increases in pollution and health impacts linked to the Salton Sea (Jones and Fleck, 2020; Jones et al., 2022). The increase in dust pollution is similar to that resulting from water transfers and agricultural diversions in Owens Lake and Great Salt Lake, as well as Lake Urmia in Iran and the Aral Sea. Furthermore, there have been regional concerns about Salton Sea-related air pollution driven by exposed playa and its environmental justice (EJ) consequences. Community groups have sought to raise awareness of the issue and local and state officials have designed conservation programs to reduce impacts.[1]

We begin by obtaining estimates of exposed playa over the period before and after water transfers began. These patches emit dust and we apply an atmospheric transport model to understand where the dust particles travel after they are released from the playa. We validate our model using pollution monitors throughout California and confirm that the movement of playa-induced dust corresponds to significant increases in measured particulate pollution (PM_{10} and $PM_{2.5}$).

We then analyze the environmental justice effects of dust-associated pollution by comparing particle exposure in disadvantaged census tracts (low-income and minority populations) to particle exposure in non-disadvantaged census tracts before and after changes in agricultural water use around the organized water transfer to San Diego. We find particles from exposed playa disproportionately affect disadvantaged communities. We test for structural breaks and find that policy changes starting in 2012 that increased exposed playa led to increased dust pollution in disadvantaged communities.

Farzan et al. (2019) state that "[t]he drying of the Salton Sea has unknown public health implications and the existing vulnerabilities of nearby populations are largely unmeasured." While some health effects associated with increased dust due to water transfers have been noted in non-academic work, the EJ implications have not been explored systematically in the academic literature. Miao et al. (2022) find that in the Coachella Valley (north of Imperial County) more vulnerable communities, as measured by a variety of indicators, are associated with higher levels

[1] In February 15, 2023, Senate Bill SB 583 was proposed to create conservation programs that could decrease pollution caused by the Salton Sea, citing health and EJ concerns.

of fine particulates. Imperial County's population is 80 percent Hispanic and 10.5 percent Black, meaning it is a community made up almost entirely of historically marginalized groups that have predominantly not been included in the political decisions to transfer the water, or in discussions of the mechanisms by which to offset negative externalities. 20 percent of children in Imperial County are estimated to have asthma versus just 8.3 percent in US population (Lipsett et al., 2009), and Imperial County has two times the rate of pediatric asthma-related emergency room visits relative to California.[2]

Several EJ studies have analyzed the role of industrial pollution processes disproportionately affecting low income and minority communities (e.g. Agyeman et al., 2016; Ard, 2015), and the availability of satellite data, crowdsourced pollution monitors, and pollution transport models have allowed researchers to study other non-industrial sources of pollution disparities (Colmer et al., 2020; Kramer et al., 2023; Tessum et al., 2019). Our paper contributes to this literature by causally linking lake bed exposure to increased dust-based air pollution and then estimating the spatial distribution of pollutants across disadvantaged populations. While the role of other non-industrial sources on pollution burdens has been evaluated (Burke et al., 2021), less is known about changes in environmental disparities due to agricultural water use and reallocation. The paper also uses a pollution transport model to link changes in pollution sources to the impacts on communities, contributing to a growing literature using atmospheric transport models to understand EJ outcomes (Cain et al., 2023).

In this setting our results show the importance of the political economy and government mechanism for inequitable EJ outcomes discussed in Banzhaf et al. (2019). Water transfer policy is largely shaped by individuals and groups with the ability to influence government, exerting pressure that may lead to less desirable outcomes for disadvantaged communities. Policies like water transfers that change property right allocations in ways that are welfare improving in aggregate may not make everyone better off, especially where contracting costs for apportioning the gains from trade are high (Libecap, 1993). In the case of the IID-San Diego transfer, a community compensation fund and an environmental mitigation fund were created, but for dollar amounts significantly less than the magnitude of the pollution externality (Ge et al., 2023).

[2]California Department of Public Health: www.cdph.ca.gov/Programs/CCDPHP/DEODC/EHIB/CPE/CDPH%20Document%20Library/County%20profiles/Imperial2016profile.pdf

2 Background

2.1 Lakebed Dust Pollution

Saline lakes contain 44% of the volume and 23% of the area of all lakes on earth (Messager et al., 2016). The drying of these lakes due to agricultural water diversions and climate change is a serious, ongoing environmental problem (Wurtsbaugh et al., 2017). Water elevation in terminal saline lakes is a balance between inflow and evaporation; saline lakes are generally shallow and can experience large areas of lakebed exposure due to small declines in water inflow. This exposed playa contains fine particles that are easily transferred via wind into dust.

Saline lakes have seen reductions in inflow as a result of agricultural and other human water diversions. Prior to an investment in dust mitigation of over $2 billion dollars by the City of Los Angeles, Owens Lake — dried due to the full diversion of the Owens River — was the largest source of particulate pollution (PM_{10}) in the United States (Kittle, 2000b). In Imperial County, airborne dust has been linked via chemical markers to Salton Sea playa (Frie et al., 2017, 2019), where soft crust playa produces significant dust during winter and early spring in processes similar to those at Owens Lake (King et al., 2011). While there is considerable variability in the emissivity of playa surfaces in the Salton Sea, newly exposed playa is particularly emissive (Dickey et al., 2023).

Dust pollution affects human health through the increase in airborne particulate concentrations of PM_{10} (diameters less than $10\mu m$) and $PM_{2.5}$ (diameters less than $2.5\mu m$). $PM_{2.5}$ particles are especially dangerous to human health, as they can make their way deep into the lungs and even bloodstream.[3] Exposure to $PM_{2.5}$ causes a variety of adverse health effects, especially related to the heart and lungs (Deryugina et al., 2019).

Atmospheric $PM_{2.5}$ due to dust storms has been shown to decrease birth weight and increase infant mortality (Jones, 2020; Heft-Neal et al., 2020). In Imperial County, decreases in Salton Sea elevation induced changes in $PM_{2.5}$ during the period 1998 to 2014, which led to serious health issues in the region (Fogel et al., 2021), including increases in respiratory mortality (Jones and Fleck, 2020).

[3] Because particles are defined according to their largest size, PM_{10} measurements are inclusive of $PM_{2.5}$.

2.2 Imperial to San Diego Water Transfer

The Salton Sea sits in Imperial County adjacent to the Imperial Irrigation District (IID). IID is the largest single user of Colorado River water, the primary water source for 40 million people in the southwestern United States. The 1922 Colorado River Compact divided 15 million acre-feet (MAF) of water between seven states, apportioning 4.4 MAF to California. Due to the use of a particularly wet baseline period and a changing climate, the estimated annual flow of the Colorado has turned out to be about 12.4 MAF, of which IID has senior rights to 3.1 MAF. In the early 2000s, California's ongoing use was in excess of its allocation, around 5.2 MAF. The 2003 transfer agreement between IID and San Diego County Water Authority (SDCWA), termed the Quantitative Settlement Agreement (QSA), was designed to help California reduce overall use.

The Salton Sea itself was created by an accidental water diversion of the entire Colorado River into Imperial County from 1905 to 1907. Because the lake has extremely limited natural inflow, it is continually replenished by the "return flows" from irrigated agriculture in IID (and to a lesser extent the nearby Coachella Irrigation District). Return flows from irrigation consist of surface water (tailwater) and underground water (drainage). Around 85% of the inflow to the Salton Sea is estimated to come from IID return flows, with around one-third (0.963 MAF) of IID's total diversions going to the lake (Jones et al., 2022). Because the majority of its inflows come from agricultural water diversions, the large reductions in water availability in the Colorado River Basin predicted under climate change (Udall and Overpeck, 2017), affect the Salton Sea indirectly, through water right allocations and their transfer.

The QSA was designed to ramp up transfers over time to 200,000 AF/year for 35 to 70 years. To provide water as stipulated in the QSA, IID began various programs to pay farmers to conserve water. From 2003 to 2011 the programs focused primarily on fallowing. Starting in 2012, the mix of programs used to generate water for transfer shifted to system efficiency measures (e.g., canal lining projects and canal seepage recovery) and on-farm efficiency measures (e.g., precision irrigation and tailwater reuse). The initial fallowing program sent a portion of conserved water directly to the Salton Sea in an attempt to offset some negative impacts. There was no mitigation program for system or on-farm efficiency programs. The net amount of water transferred (total transfer less mitigation water) is shown in the right axis of figure 1.

Figure 1: Cumulative Water Transfers and Playa Exposure

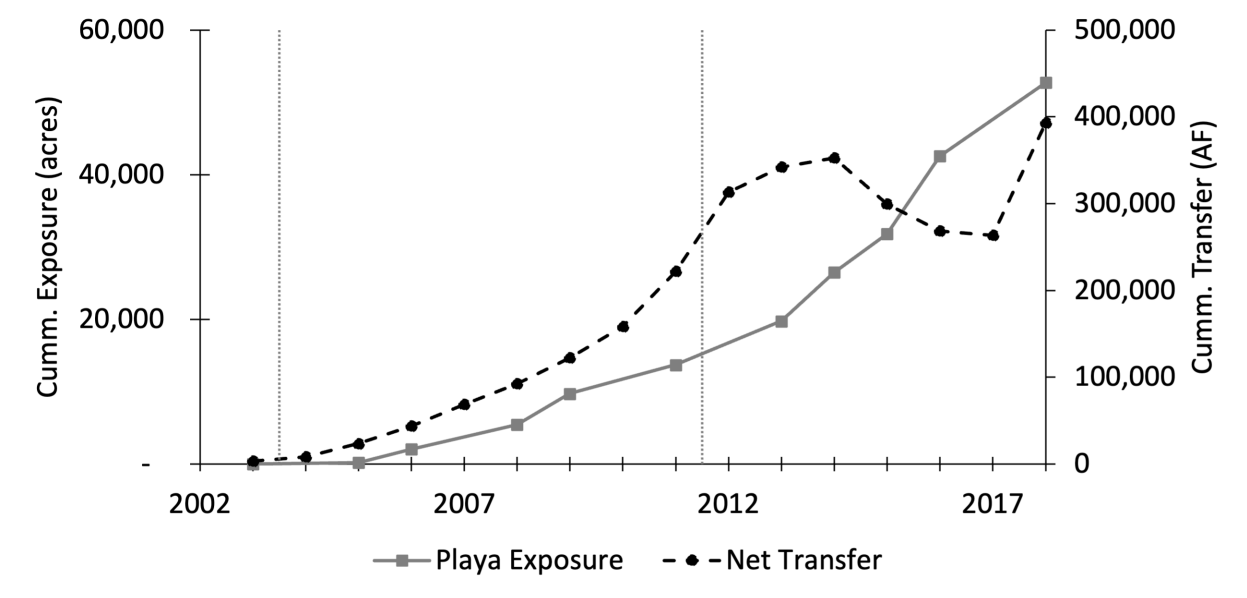

Notes: Cumulative playa exposure in acres on left-axis and cumulative net IID to SDCWA water transfer in acre-feet (water transferred minus water conserved for direct flow into Salton Sea) on right axis. Vertical lines in 2003 and 2011 show the start of the transfer program and start of intensification, respectively. Playa exposure data from Formation Environmental (2019a, 2020a, 2021a, 2022a, 2016, 2018, 2019b, 2020b, 2021b, 2022b). Water transfer data from Imperial Irrigation District (2021).

The result of the transfers was a decline in inflows to the Salton Sea (Fogel et al., 2021, p.22). In 2003, the elevation of the Salton Sea was around 229 feet below sea level (Formation Environmental, 2016). It remained about this level until 2009 when it began to decline; by the end of 2011 the elevation was around 230 feet below sea level and by 2018, the end of our sample, lake elevation had fallen to over 234 feet below sea level (Formation Environmental, 2016, 2022a).[4] As flows into the lake decreased, additional playa was exposed, especially after 2011. The annual area of playa exposed is shown in the left axis of figure 1. Every year after 2011 saw more playa exposed than in any year before 2011. New playa exposure in just 2017 and 2018 exceeded the total area exposed prior to 2012.

The Imperial Valley community, made up of predominantly Latino agricultural workers and Indigenous tribes, was largely absent from the water transfer decision making process due to the lack of political power in rural communities, short-term planning, and limited community engagement (Johnston et al., 2019). Nonetheless, two programs emerged with the QSA to mitigate environmental and economic impacts associated with the transfer program: the Local Entity and

[4]Elevation reports by Formation Environmental (2016, 2022a) differ somewhat from average elevation data gathered from USGS gauge "Salton Sea NR Westmorland CA - 10254005" as shown on figure 2, likely due to within-year fluctuations in water level. The pattern of decline, however, is consistent across both measures.

the Salton Sea Air Quality Mitigation Program. The Local Entity was created to quantify and offset third-party socio-economic impacts of fallowing under the program. In 2007, IID and SDCWA agreed to make $50 million available to mitigate impacts within the IID water service area ($30 million provided by SDCWA and $20 million by IID). To date, $32 million in mitigation funding has been made available to farm service providers, $11 million to community business endeavors, and $6 million for special projects, including reopening a beef processing plant and developing a sugarcane processing plant.

The Air Quality Mitigation Program was set up in 2003 and requires IID and SDCWA, along with Coachella Valley Water District, to provide up to $133 million (in 2003 dollars) to pay for environmental mitigation costs. The program monitors and models playa dust emissions and implements dust control mitigation. As of its October 2023 report, the Program had implemented projects mitigating dust on 7,001 acres, with 7,628 acres in active planning and another 2,438 identified as priority areas for future proactive dust control (Formation Environmental, 2023).

There is considerable uncertainty about how emissive playa surfaces in the Salton Sea are (King et al., 2011). Dickey et al. (2023) states that there is "an almost 20-fold reduction in PM_{10} emission potential between the dry and moist soil classes and a 7-fold reduction between the dry and slightly moist soil class." Because we lack a systematic spatial assessment of playa emissivity over time at a fine resolution, the remainder of the paper utilizes an intent-to-treat approach. Exposed playa is a key potential source of dust, and so we allow the data to tell us whether particles from these areas are increasing air pollution.

3 Data

Salton Sea water elevation: We obtained Salton Sea exposed playa locations by collecting lake and lakebed elevation data. We generated a 1 km $\times$ 1 km grid for an area around the 2002 and 2018 lake shoreline, as derived from shapefiles created by the Imperial Irrigation District Salton Sea Air Quality Mitigation Program.[5] After obtaining the centroid of each grid cell, we found the lakebed elevation by matching each centroid to the closest Salton Sea bathymetry contour (one foot) from

[5] https://saltonseaprogram.com/aqm/data-portal/data-portal.php

the California Department of Fish and Wildlife.[6] We then compared the water level — using the elevation of the lake from United States Geologic Survey gauge 10254005 — with the elevation of the exposed playa, providing an estimate of annual time-varying playa exposure, as shown in figure 2. For the remainder of the paper we refer to these centroids as playa points.

Figure 2: Salton Sea Playa Exposure through 2018

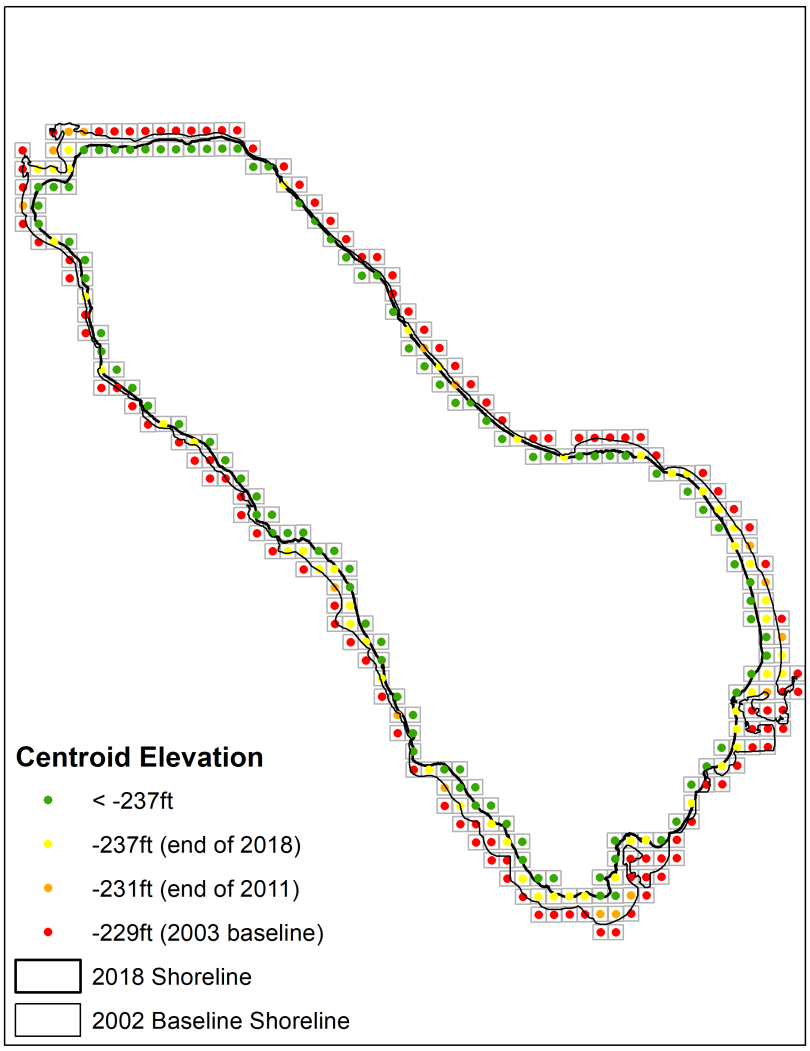

Notes: This figure presents the point grids and associated centroids used to model the atmospheric transport model. The figure shows the estimates of annual-time-varying playa exposure per date of exposure.

Particle transport: To model dust pollution from playa points we use the Hybrid Single Particle Lagrangian Integrated Trajectory Model (HYSPLIT), an atmospheric dispersal model devel-

[6] https://gis.data.ca.gov/datasets/30ab3e1e70824f21b1136d3296cf17f4/explore?location=33.313653%2C-115.832324%2C11.24

oped by the U.S. National Oceanographic and Atmospheric Administration with real-time meteorological conditions from NOAA's 40-km resolution North American Model Data Assimilation System (Draxler and Hess, 1998). To obtain particle trajectories, we apply the HYSPLIT model to each playa point . We model forward trajectories (i.e. consider a particle released from the location in question and follow it over time) from ground-level released particles. We obtain two trajectories for each day, one at 6 AM and one at 6 PM. The HYSPLIT model provides elevation and coordinates of the particle for every hour following the initial release. Figure A1 provides examples of these trajectories originating from one individual playa location. Distance, direction, and elevation are determined by time and location-specific meteorological data.

Unlike other HYSPLIT applications that link locations with estimated emissions via emissions inventories or other data sources (e.g. Grainger and Ruangmas, 2018; Hernandez-Cortes and Meng, 2023), we do not model actual emissions from the source. Other studies have obtained measures of total PM emissions from the Salton Sea, for example, Jones et al. (2022) obtained the PM_{10} emissions relative to 2016 by using information on the total exposed area, emissions factors, and a modeling approach developed by MacDougall and Uhl (2002). However, obtaining twice daily emissions of each exposed playa location to match the time resolution of the atmospheric transport model (two releases daily for 1998-2018) would require detailed information on total emissions in each location we examine, data that occur at too high a resolution and frequency to be measured directly.[7] Because estimating location-specific contributions to pollution (i.e. playa point contributions to pollution in a specific spatial location) requires high spatial and temporal resolution data, we choose to instead model particle paths, twice daily 'particle releases' from each playa point, and follow their trajectories. We do not observe concentrations, but instead observe what we define as a particle-hour: the total number of hours a particle from an exposed playa point is within a buffer around a monitor, or alternatively, within a census tract. This measure is similar to the one used by Heo et al. (2023), who calculates the percentage of hours that particles in South Korea are coming from China.

We only consider particles that have a height of 1 km or less, which is within estimates of California's boundary layer (Rahn and Mitchell, 2016).[8] While the particles could travel beyond

[7] An alternative approach would model these emissions, but this would unnecessarily introduce measurement error.
[8] As a robustness check, we show that our results do not change when using 0.5 km as maximum height.

California, we focus our analysis in California because most of the environmental justice concerns related to the Salton Sea have been related to California communities and most of the larger populations near the Salton Sea are located in California. However, examining the environmental justice consequences in other areas such as Arizona, Nevada, and northern Mexico is important for future work.

Pollution monitor data: We use pollution monitor data from the EPA, which provides the location of all pollution monitoring stations in California. We obtained daily data on PM_{10} concentrations ($\mu g/m^3$) for 1998 to 2018, and $PM_{2.5}$ concentrations ($\mu g/m^3$) in three-day increments from 1998-2002 and then daily from 2002.[9] We use the monitor data to understand whether particles released from the Salton Sea are associated with larger pollution concentrations. To do this, we create 5-km buffers surrounding all California monitors and spatially merge them to particle trajectories from HYSPLIT. Appendix figure A2 shows the location of the monitors in the sample which experience at least one particle-hour measured during the 1998-2017. Monitors with particles are generally located in Southern California, with a few of them covering parts of Central and Northern California.

Socioeconomic vulnerability: We use the CalEnviroScreen 4.0 (CES4.0) definition of "Disadvantaged Community (DAC)." The CES4.0 considers several socioeconomic and health indicators to construct a score at the census tract level. Census tracts receiving the highest 25 percent of overall scores in CalEnviroScreen are deemed to be DAC.[10] We obtain alternative measures of vulnerable community status, linguistic variation and poverty, from the raw data used to construct the CES4.0. Table 1 shows the descriptive statistics by census tract bifurcated by whether the tract is transited by a playa particle during the study period (column 1) or sees zero particles (column 2), as well as the difference in means (column 3).

The purpose of this table is to provide descriptive statistics of the areas that show positive particle-hours compared to areas without particle-hours. The annual total particle-hours is the average number of particle-hours from all emitted sources at the census tract level calculated using HYSPLIT. The rest of the variables were obtained from CES4.0 indicators. Census tracts with

[9] https://www.epa.gov/outdoor-air-quality-data/download-daily-data
[10] https://oehha.ca.gov/calenviroscreen/sb535

Table 1: Descriptive Statistics

	(1) More than zero particle-hours	(2) Zero particle-hours	(3) Difference
Annual particle-hours	825.892	0.000	825.892**
	(16019.98)	(0.00)	(3.272)
Population (2019)	5110.279	4750.580	359.699***
	(2411.35)	(2023.13)	(7.190)
Ozone (max 8 hr concentration)	0.053	0.044	0.009***
	(0.01)	(0.01)	(41.777)
Annual PM2.5 concentrations	10.992	9.304	1.687***
	(1.84)	(2.14)	(37.689)
Disadvantaged community (% census tracts)	0.281	0.218	0.063***
	(0.45)	(0.41)	(6.499)
Poverty above 75th percentile (% census tracts)	0.257	0.243	0.014
	(0.44)	(0.43)	(1.481)
Linguistic isolation above 75th percentile (% census tracts)	0.245	0.239	0.006
	(0.43)	(0.43)	(0.591)
Observations	4008	4028	8036

Notes: This table shows descriptive statistics at the census tract level divided by number of affected particle hours during the 1998-2017 time period. Column (1) shows the mean and standard deviation for census tracts that experience positive particle hours during 1998-2017. Column (2) shows the mean and standard deviation for census tracts that experienced zero particle hours during 1998-2017. Column (3) shows the results of the two-sample mean-comparison test using the two groups in columns (1) and (2) with the corresponding t statistics in parenthesis below. Annual particle hours are obtained from HYSPLIT and correspond to 1998-2017. Total population was obtained from CES4.0 and corresponds to 2019 census data. Ozone (maximum 8 hr concentration) was obtained from CES4.0 and corresponds to the average maximum levels during the period 2017-2019 from the Air Quality Monitoring Network, California Air Resources Board. Annual $PM_{2.5}$ concentrations were obtained from CEs4.0 and correspond to the annual mean concentration over the period 2015-2017 from the Air Quality Monitoring Network, California Air Resources Board. Disadvantaged community (% of census tracts) was obtained from CES4.0, which provides the percentiles of the CES4.0 and communities were classified as disadvantaged if their score is located among the highest 25 percent of overall scores in CES4.0. Poverty above 75th percentile was calculated from data in the CES4.0 and corresponds to the percent of the population living below two times the federal poverty level (5-year estimate, 2015-2019) from the ACS. Linguistic isolation above 75th percentile was calculated from data in the CES4.0 and corresponds to the percentage of limited English-speaking households (5-year estimate, 2015-2019) from the ACS.

more than zero particle-hours have higher average populations than census tracts with zero particles. Both Ozone and $PM_{2.5}$ are higher in census tracts with more than zero particle-hours, and the difference is statistically significant. Furthermore, the share of census tracts classified as disadvantaged is higher in areas with more than zero particle-hours. However, poverty and linguistic isolation measures are relatively similar between census tract types, and these differences are not statistically significant. Figure 3 shows the spatial pattern of total playa dust particles transiting census tracts. Census tracts receiving at least some particles tend to be located closer to the Salton Sea, with relatively higher particle counts to the east.

Figure 3: Average Exposure to Particle-Hours by Census Tract

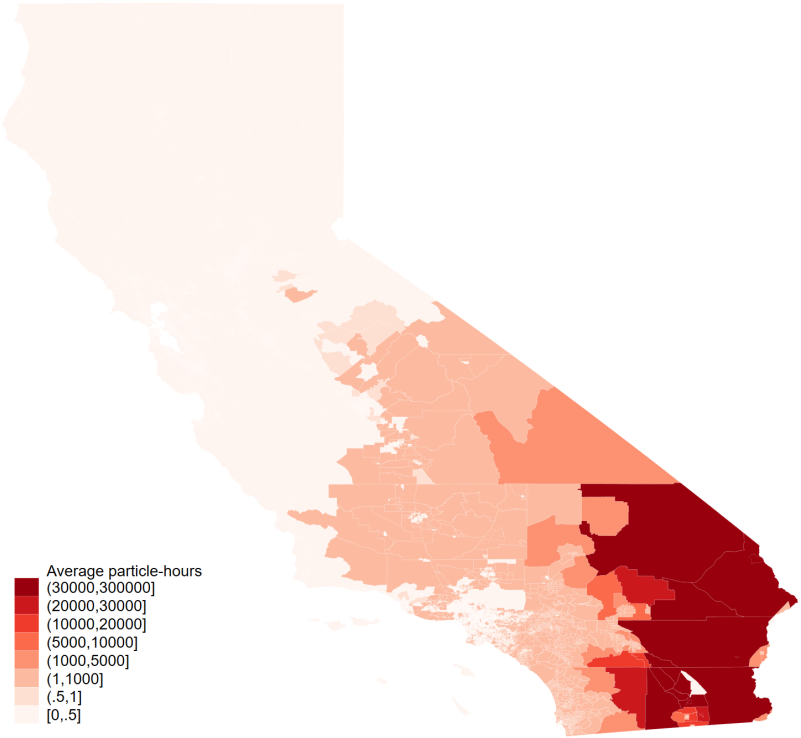

Notes: This figure presents the average particle-hours exposure at the census tract from all contributing playa points for the period 1998-2017 in California. Particle-hour exposure was modeled using HYSPLIT, restricting to particles within a boundary layer of 1,000m. Census tracts are based on 2010 cartography, obtained from the CES4.0.

4 Empirical Strategy

Our empirical approach links the increasing playa area of the Salton Sea to air pollution from dust and its distribution across communities. We do so by (1) applying the atmospheric transport model described above to track particles emitted at a particular spatial location and time as they travel due to atmospheric conditions; (2) validating this model by linking these particle transport trajectories to air pollution monitors and demonstrating a robust relationship between our measure of 'particle hours' and observed PM_{10} and $PM_{2.5}$ concentrations; and (3) tracking the concentration of particle destinations over time to different census tracts and distinguishing between disadvantaged and other communities.

The meteorological transport model and the timing of exposed playa due to the falling elevation of the Salton Sea provide sources of variation for particle exposure. Because we include the trajectories from locations only when the elevation of the lake drops below the elevation of each playa centroid, throughout our sample period the number of particle-emitting locations increases. Figure A3 shows the total number of particle hours over the time period for all census tracts in California. The number of particles are increasing over time mechanically, as more playa points are exposed, but there is also annual variation due to meteorological conditions. For instance, between 2004 and 2011 we observe a relative decline in particle hours due to meteorological conditions that caused particles to exit California census tracts more quickly. From 2012 onward we see an increase in particle hours as more playa locations become exposed due to increasing playa exposure.

Because we do not observe playa emissivity, the same number of particle paths exist for each exposed playa point. This presents two concerns. The first is whether the particle-hours measure is indeed associated with higher pollution concentrations on the ground (i.e. is the exposed playa surface actually emitting enough dust to affect air quality throughout California?). The second is whether particle hours emerging from different playa points can be aggregated, as they may be indicative of different concentrations of pollution due to differing cell emissivity.

To address these concerns, we test whether emissions correspond to recorded pollution concentrations by linking pollution monitor data with the modeled particle trajectories at the monitor-playa point-day. We count the number of modeled particle-hours in the 5 km buffer around each

monitor each day for each playa point. We then regress both PM_{10} and $PM_{2.5}$ concentrations on the number of particles in the monitors' buffers using the following model:

$$y_{ikdmt} = \beta T_{ikdmt} + \gamma_{ik} + \mu_t + \theta_m + u_{ikdmt} \tag{1}$$

In the above equation i indexes a specific monitor (destination); k the specific playa point (source); d, m, and t index day, month, and year respectively. The outcome variable y_{ikdmt} is the monitor-specific reading of PM_{10} and $PM_{2.5}$ in a given day and the explanatory variable of interest is T_{idmt}, the number of particle-hours measured in the monitor's buffer that day coming from a playa point k.

The coefficient β captures the relationship between the total particles and the PM concentrations and provides our test of the transport model. β should be interpreted as the average across all playa point-monitor combinations of the impact of an additional particle hour from a particular playa point. Small and statistically insignificant estimates would indicate that the HYSPLIT-modeled particulate paths have little relationship to ambient PM concentrations. Significant positive estimates, however, indicate that the modeled particulates increase PM concentrations.

We include monitor by playa point fixed effects, year fixed effects, and month fixed effects and provide robustness checks for day-of-week fixed effects. Monitor-by-playa point fixed effects, γ_{ik}, control for time-invariant unobservable factors that influence average pollution monitor readings, the average effect a particular playa point has on all pollution, and the pairwise effect of each playa point on each monitor. This approach ensures that our coefficient estimates of β are only coming from the explicit modeling of the HYSPLIT trajectories and not being driven by other factors.[11] All standard errors are clustered at the monitor level.

Validating that the transport model links particle hours to actual increases in monitor pollution measurements justifies subsequent tracking of particle hours in aggregate across playa points as they transit different census tracts. We plot trends in pollution exposure (via modeled particles) for different DAC categories and test whether trends or differences in trends change around 2011 when additional water transfers via on-farm and system conservation measures began. We consider

[11] The source-by-destination fixed effect captures the unobservable average effects a particular playa point may have on ambient pollution for each monitor individually, rather than simply including playa point fixed effects which would account for the average effect of that each playa point has on all pollution monitors — some of which might be close and others far away.

changes in particles that arise from the increasing number of playa points and atmospheric factors. Because our outcome is the number of particle hours in a given census tract in a given month, and many of these values are zero, we use a Poisson model to estimate the following trend break model:

$$\mathbb{E}[p_{jtm}|t, j, m] = exp\{\tau \times t + \rho I_{t>2011} \times t + \lambda I_{t>2011} + \sigma_j + \psi_m\} \tag{2}$$

Where the outcome p_{jtm} is the number of particle-hours in a census tract j in month m of year t. $I_{t>2011}$ is an indicator for post-2011, σ_j captures census tract effects, ψ_m denotes month-of-year fixed effects to control for seasonality, and t is a linear time trend in year. A positive coefficient estimate for ρ indicates that there is a change in trend post 2011; we run with a combined set of tracts as well as DAC and non-DAC tracts separately to understand changing trends. We present results from these exercises in the following section.

5 Results

5.1 Particulate Pollution

We first analyze whether an increase in the number of particle-hours modeled with HYSPLIT increases pollution levels using equation 1. Table 2 shows these results for PM_{10} (columns 1-3) and for $PM_{2.5}$ (columns 4-6). We find that an increase of one particle-hour increases PM_{10} concentrations by 1.269 (2.93%) and increase $PM_{2.5}$ concentrations by 7.57%. Table A1 shows the same specification restricting particle height to be 500 meters, which is similar to sensitivity analyses to different boundary layers in California (Rahn and Mitchell, 2016; Hernandez-Cortes and Meng, 2023).

We present several robustness checks for this result. We estimate equation 1 with additional weather controls that can affect pollution outcomes at the monitors such as maximum air temperature, precipitation amount, wind speed, and specific humidity. We obtain these data from gridMET, a dataset that contains daily meteorological information on a 4km $\times$ 4km resolution.[12] Table A2

[12]We obtained these weather controls by overlapping the location of the pollution monitors in the gridMET product and obtained the daily average observation for each of the meteorological variables.

shows results with these additional weather controls, which are similar in magnitude to our main specification, albeit with some differences. For example, we find larger effects for PM_{10} but the coefficients for $PM_{2.5}$ are smaller. In all specifications, however, our measure of particle hours remains significant at the 5% confidence level.

Additionally, we expect precipitation near the Salton Sea to temporarily reduce emissivity of the exposed playa. We validate this in two ways: 1) we restrict our analysis to days without rain and 2) we estimated a similar equation to 1 adding an indicator variable on whether there was any rain that day at the Salton Sea (both of these analyses use data from a weather monitoring station close to the Salton Sea).[13] Tables A3 and A4 show these results. Table A3 restricts the regressions to days without rainfall at the Salton Sea and Table A4 interacts total particle-hours with an indicator variable if there was rainfall recorded at the Salton Sea. Both tables show results consistent with reduced emissions from the Salton Sea on days with rainfall.

Finally, we compare our analysis to monitors close to the Salton Sea and monitors farther from the Salton Sea. We calculate the Euclidean distance from each monitor to the Salton Sea and estimate equation 1 for monitors within 100 miles and monitors farther than 100 miles.[14] Table A5 shows stronger effects for monitors within 100 miles from the Salton Sea (Panel a) compared to monitors farther than 100 miles from the Salton Sea (Panel b), where no coefficient is significant.

These results provide important validation of our particulate transport model. Despite the absence of data on actual source emissions discussed above, the modeled particulate transport has a significant relationship with ambient pollution concentrations.

5.2 Exposed Playa and Environmental Justice Outcomes

We now turn our attention to the spatial distribution of the dust emitted from the Salton Sea playa. Figure 3 shows the average total number of particle-hours in each census tract from Salton Sea playa points from 1998 to 2017. Most of the effects are concentrated in the eastern portion of Southern California (areas of Imperial, Riverside, and San Bernardino counties). Some areas of

[13]The station is Calipatria/Mulberry - Imperial/Coachella Valley - Station 41, which was the closest station and the one with the longest temporal coverage.

[14]Particulate matter can travel for several miles from where it is emitted. While our atmospheric transport model accounts for the pollution transport from sources to receptors, we followed Barreca et al. (2017) and compared monitors within 100 miles from the Salton Sea and monitors farther than 100 miles from the Salton Sea.

Table 2: Exposed Playa and Pollution Outcomes

	(1) PM_{10}	(2) PM_{10}	(3) PM_{10}	(4) $PM_{2.5}$	(5) $PM_{2.5}$	(6) $PM_{2.5}$
Total particles	1.269***	1.370***	1.406***	0.817***	0.766***	0.764***
	(0.325)	(0.282)	(0.283)	(0.199)	(0.199)	(0.199)
Mean	43.222	43.222	43.222	10.785	10.785	10.785
Obs.	265,093	265,093	265,093	231,768	231,768	231,768
R-squared	0.112	0.139	0.153	0.257	0.285	0.289
Year FE	Yes	Yes	Yes	Yes	Yes	Yes
Month FE	No	Yes	Yes	No	Yes	Yes
Site by point FE	Yes	Yes	Yes	Yes	Yes	Yes
Day of week FE	No	No	Yes	No	No	Yes
Cluster level	Site	Site	Site	Site	Site	Site

Notes: Above are coefficient estimates of β from Equation (1). Columns (1) through (3) use PM_{10} concentrations and Columns (4) through (6) use $PM_{2.5}$ as outcome variables. Fixed effects are indicated by column labels and all standard errors are clustered at the monitor level. The mean indicates the average pollution concentration for the respective pollutant. Particles restricted to a boundary layer of 1,000m.

Los Angeles and San Diego counties are also affected. However, coastal areas of Southern California and most of Northern California have zero modeled particle-hours.

In order to analyze the impacts of increases in exposed playa on environmental justice outcomes, we first show that total particle-hours increased after 2011, consistent with the increases in exposed playa shown in figure 1. Figure 4 shows the annual average number of total particle-hours from exposed playa points for both disadvantaged and other communities. Disadvantaged communities experience a higher average number of particle-hours during most of the 1998-2017 period. Pre-2012, there are some fluctuations in year-to-year number of particle-hours. However, after 2011, the number of particles increase in disadvantaged communities, while the number of particle-hours in non-disadvantaged communities stayed relatively constant, with some increases at the end of the study period.

We estimate these differences using other measures that have been used in the environmental justice literature as indicators of social and economic vulnerability: poverty and linguistic isolation. Figure A4 shows these results. Panel a) shows differences by poverty level (communities in the top 25th poverty percentile in blue and the rest of the communities in orange) and Panel b) shows differences by linguistic isolation (communities in the top 25th percentile of linguistic isolation in blue and the rest of the communities in orange). Both figures show that communities with higher

levels of vulnerability have higher levels of particle-hour exposure, consistent with the results in figure 4.

Figure 4: Exposure to Particle-Hours by Disadvantaged Status

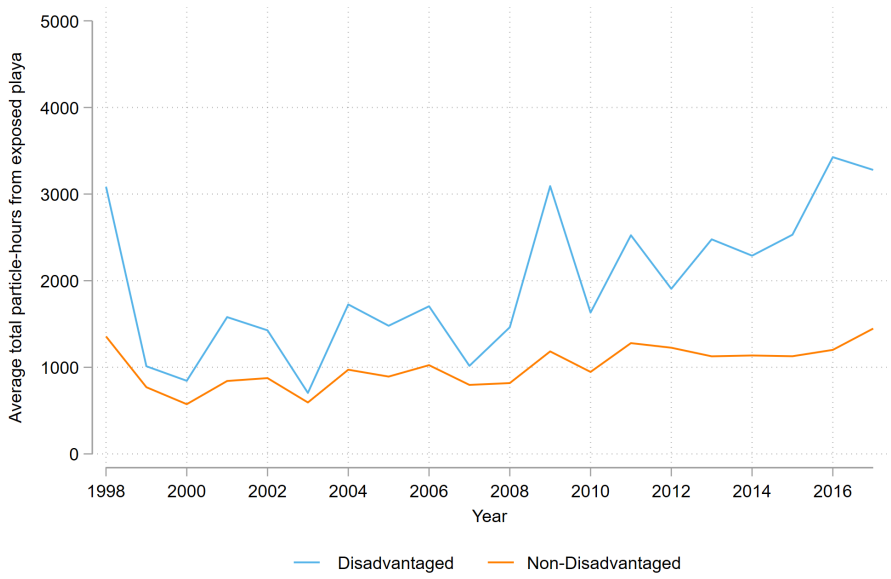

Notes: This figure presents the average particle-hours exposure for the period 1998-2017 in California for Disadvantaged (blue) and non-disadvantaged (orange) communities. Particle-hour exposure was modeled using HYSPLIT. Particles restricted to a boundary layer of 1,000m. Disadvantaged communities classification was obtained from CES4.0.

We formalize these findings in figure 5 by estimating a Poisson model (with both census tract and year-fixed effects) and plot the year fixed effects estimates relative to a 2011 baseline, where the dependent variable is the number of total particle-hours. We estimate this model for all communities (Panel A) and separately for disadvantaged communities (Panel B) and other communities (Panel C). Panel D interacts year-specific coefficients with an indicator variable on whether the community is disadvantaged. Panel A shows that before 2011, there were no differences in total particle-hours exposure, however, we see an increase after 2011. Panel B shows that before 2011 there are only statistically significant differences in total particles in one year. After 2011, there is a constant increase on average particle-hours in DAC communities. This pattern is not present when we restrict our sample to non-DAC communities (Panel C), suggesting the post-2011 increase in Panel A is due to increases in DAC communities. Panel D confirms the difference between DAC and non-DAC communities, although there are some statistically significant differences prior to

Figure 5: Difference in Total Particles Relative to 2011

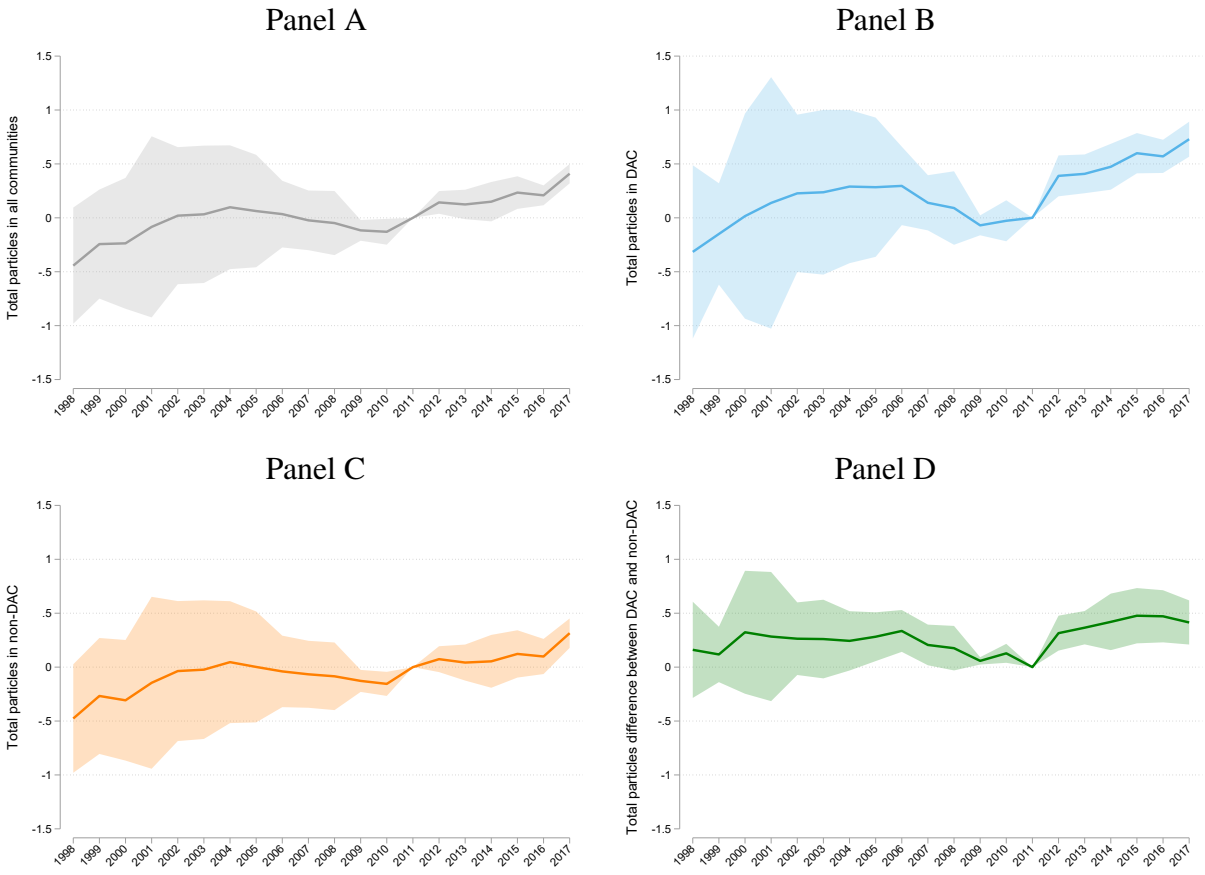

Notes: This figure presents the annual difference in particle-hours exposure for the period 1998-2017 in California for all communities (Panel a), Disadvantaged communities (Panel b) and non-disadvantaged communities (Panel c). Panel d shows the interaction between year and disadvantaged communities indicator. Particle-hour exposure was modeled using HYSPLIT. Disadvantaged communities classification was obtained from CES4.0. Census tracts are based on 2010 cartography, obtained from the CES4.0. Particles are restricted to have a maximum height of 1000 meters.

2011.

To examine whether there is a statistically meaningful trend break after 2011, we estimate equation 2 for the entire time period (columns 1-3 in table 3) and the post-2003 period following the enactment of the QSA (columns 4-6 in table 3). We show results for all communities (columns 1 and 4), for DAC communities (columns 2 and 5), and for non-DAC communities (columns 3 and 6). The main coefficient of interest, ρ, shows that after 2011 and accounting for existing trends, disadvantaged communities experienced an increase in the number of particle-hours. The change in trend exists using data from the entire time period and restricting the data for the period 2003-2017. Consistent with the results in figures 4 and 5, results from columns 2 and 5 suggest that

Table 3: Trend-Break Model

	(1) All	(2) DAC	(3) Other	(4) All	(5) DAC	(6) Other
Trend × post 2011	0.037	0.080***	0.022	0.084*	0.143***	0.065
	(0.02513)	(0.02762)	(0.03027)	(0.04330)	(0.04365)	(0.04931)
Post 2011	-0.021	-0.006	-0.024	0.170***	0.250***	0.148***
	(0.05132)	(0.05914)	(0.05580)	(0.04738)	(0.06626)	(0.04850)
Trend	0.017	0.012	0.018	-0.031	-0.050	-0.025
	(0.02207)	(0.02972)	(0.02123)	(0.04024)	(0.04806)	(0.04005)
Mean	35.492	33.882	36.037	39.292	38.775	39.462
Obs.	825,360	208,560	616,800	594,720	146,700	448,020
Census tract FE	Yes	Yes	Yes	Yes	Yes	Yes
Cluster level	County	County	County	County	County	County
Period	1998-2017	1998-2017	1998-2017	2003-2017	2003-2017	2003-2017

Notes: This table shows the results for equation (2) separately for All (columns 1 and 4), Disadvantaged (columns 2 and 5) and non-Disadvantaged (columns 3 and 6) communities. Columns 1-3 show the results for the entire study period and Columns 4-6 show the results for the 2003-2017 period. Disadvantaged communities classification was obtained from CES4.0. Particles restricted to have a maximum height of 1,000 meters.

the increasing trend in the total particle-hours after 2011 is occurring in DAC communities. We estimate that on average, DAC communities experienced 8.32% additional total particles per year after 2011 for the 1998-2017 period or 15.37% additional total particles per year after 2011 for the 2003-2017 period relative to the pre-2011 trends.[15] Table A6 shows the results restricting to particles with height lower than 500m as a robustness check. The results are similar in magnitude to the results in table 3.

6 Conclusion

Water diversions for agriculture pose significant risks to the environment and public health when they lead to reduced lake levels and increased dust pollution in downwind communities. This paper examines whether dust pollution from changing patterns of agricultural water use increases environmental disparities for a large water transfer in Southern California. We find that transfers from the Imperial Irrigation District to San Diego County increased pollution in disadvantaged communities, overall and relative to non-disadvantaged communities.

[15] Using the coefficients from specification (2) in table 3: $e^{0.080} - 1$=0.0832 for 1998-2017 and $e^{0.143} - 1$=0.1537 for 2003-2017.

Using an atmospheric transport model linking exposed lakebed after the water transfer to patterns of dust pollution, we show that lakebed dust increases the number of particle-hours and PM_{10} and $PM_{2.5}$ pollution levels around monitoring stations. Given that the Salton Sea is located in a rural area near low-income and predominantly minority communities, we examine which communities experienced an increase in total particle-hours after 2011, when changes in the water transfer program exposed additional lakebed playa. We find that the number of particle-hours coming from exposed playa disproportionately increased in disadvantaged communities, and we find that non-disadvantaged communities did not experience an increase in particle-hours exposure. While the surrounding historically disadvantaged communities consistently experienced higher pollution exposure from the Salton Sea dust, the pollution exposure gap between disadvantaged and non-disadvantaged communities grew appreciably following the changes in agricultural water use from the water transfer. As water transfer policy is largely shaped by individuals and groups with influence in the policy-making process, those who have historically not participated in these processes may disproportionately bear the negative environmental consequences. These results suggest the need for distributional analyses in water transfer programs to evaluate and potentially compensate disadvantaged communities for negative external effects.

References

Agyeman, Julian, David Schlosberg, Luke Craven, and Caitlin Matthews, "Trends and directions in environmental justice: from inequity to everyday life, community, and just sustainabilities," *Annual Review of Environment and Resources*, 2016, *41*, 321–340.

Ard, Kerry, "Trends in exposure to industrial air toxins for different racial and socioeconomic groups: A spatial and temporal examination of environmental inequality in the US from 1995 to 2004," *Social Science Research*, 2015, *53*, 375–390.

Banzhaf, Spencer, Lala Ma, and Christopher Timmins, "Environmental justice: The economics of race, place, and pollution," *Journal of Economic Perspectives*, 2019, *33* (1), 185–208.

Barreca, Alan I, Matthew Neidell, and Nicholas J Sanders, "Long-run pollution exposure and adult mortality: Evidence from the acid rain program," Technical Report, National Bureau of Economic Research 2017.

Burke, Marshall, Anne Driscoll, Sam Heft-Neal, Jiani Xue, Jennifer Burney, and Michael Wara, "The changing risk and burden of wildfire in the United States," *Proceedings of the National Academy of Sciences*, 2021, *118* (2), e2011048118.

Cain, Lucas, Danae Hernandez-Cortes, Christopher Timmins, and Paige Weber, "Recent Findings and Methodologies in Economics Research in Environmental Justice," 2023.

Colmer, Jonathan, Ian Hardman, Jay Shimshack, and John Voorheis, "Disparities in PM2. 5 air pollution in the United States," *Science*, 2020, *369* (6503), 575–578.

Deryugina, Tatyana, Garth Heutel, Nolan H Miller, David Molitor, and Julian Reif, "The Mortality and Medical Costs of Air Pollution: Evidence from Changes in Wind Direction," *American Economic Review*, 2019, *109* (12), 4178–4219.

Dickey, Hank, Maarten Schreuder, Brian Schmid, and Yohannes T Yimam, "Quantifying dust emission potential of playa and desert surfaces in the Salton Sea Air Basin, California, United States," *Aeolian Research*, 2023, *60*, 100850.

Draxler, Roland R and GD Hess, "An overview of the HYSPLIT_4 modelling system for trajectories," *Australian meteorological magazine*, 1998, *47* (4), 295–308.

D'Odorico, Paolo, Davide Danilo Chiarelli, Lorenzo Rosa, Alfredo Bini, David Zilberman, and Maria Cristina Rulli, "The global value of water in agriculture," *Proceedings of the national academy of sciences*, 2020, *117* (36), 21985–21993.

Farzan, Shohreh F, Mitiasoa Razafy, Sandrah P Eckel, Luis Olmedo, Esther Bejarano, and Jill E Johnston, "Assessment of respiratory health symptoms and asthma in children near a drying saline lake," *International Journal of Environmental Research and Public Health*, 2019, *16* (20), 3828.

Fogel, Marilyn, Hoori Ajami, Emma Aronson, Roya Bahreini, Wilfred Elders, Darrel Jenerette, David Lo, Timothy Lyons, Michael McKibben, William Porter, Arun Raju, Kurt Schwabe, Caroline Hung, and Jonathan Nye, "Crisis at the Salton Sea: The Vital Role of Science," 2021. The EDGE Institute, University of California Riverside, Salton Sea Task Force.

Formation Environmental, "Salton Sea Air Quality Mitigation Program," Technical Report, Prepared for Imperial Irrigation District 2016.

_ , "Salton Sea Emissions Monitoring Program: 2016/2017 Annual Report and Emissions Estimates," Technical Report, Prepared for Imperial Irrigation District 2018.

_ , "END-OF-YEAR 2018 PLAYA EXPOSURE ESTIMATE," Technical Report, Prepared for Imperial Irrigation District 2019.

_ , "Salton Sea Emissions Monitoring Program: 2017/2018 Annual Report and Emissions Estimates," Technical Report, Prepared for Imperial Irrigation District 2019.

_ , "END-OF-YEAR 2019 PLAYA EXPOSURE ESTIMATE," Technical Report, Prepared for Imperial Irrigation District 2020.

_ , "Salton Sea Emissions Monitoring Program: 2018/2019 Annual Report and Emissions Estimates," Technical Report, Prepared for Imperial Irrigation District 2020.

_ , "END-OF-YEAR 2020 PLAYA EXPOSURE ESTIMATE," Technical Report, Prepared for Imperial Irrigation District 2021.

_ , "Salton Sea Emissions Monitoring Program: 2019/2020 Annual Report and Emissions Estimates," Technical Report, Prepared for Imperial Irrigation District 2021.

_ , "END-OF-YEAR 2021 PLAYA EXPOSURE ESTIMATE," Technical Report, Prepared for Imperial Irrigation District 2022.

_ , "Salton Sea Emissions Monitoring Program: 2020/2021 Annual Report and Emissions Estimates," Technical Report, Prepared for Imperial Irrigation District 2022.

_ , "Salton Sea Air Quality Mitigation Program: Proactive Dust Control Plan for 2022 / 2023," Technical Report 2023.

Frie, Alexander L, Alexis C Garrison, Michael V Schaefer, Steve M Bates, Jon Botthoff, Mia Maltz, Samantha C Ying, Timothy Lyons, Michael F Allen, Emma Aronson et al., "Dust Sources in the Salton Sea Basin: A Clear Case of an Anthropogenically Impacted Dust Budget," *Environmental Science & Technology*, 2019, *53* (16), 9378–9388.

Frie, Alexander L., Justin H Dingle, Samantha C. Ying, and Roya Bahreini, "The Effect of a Receding Saline Lake (the Salton Sea) on Airborne Particulate Matter Composition," *Environmental Science & Technology*, 2017, *51* (15), 8283–8292.

Ge, Muyang, Sherzod B Akhundjanov, Eric C Edwards, and Reza Oladi, "Left in the Dust? The Agricultural and Environmental Costs of Rural-Urban Water Sales," 2023.

Grainger, Corbett and Thanicha Ruangmas, "Who wins from emissions trading? Evidence from California," *Environmental and resource economics*, 2018, *71*, 703–727.

Heft-Neal, Sam, Jennifer Burney, Eran Bendavid, Kara K Voss, and Marshall Burke, "Dust pollution from the Sahara and African infant mortality," *Nature Sustainability*, 2020, *3* (10), 863–871.

Heo, Seonmin Will, Koichiro Ito, and Rao Kotamarthi, "International spillover effects of air pollution: evidence from mortality and health data," Technical Report, National Bureau of Economic Research 2023.

Hernandez-Cortes, Danae and Kyle C Meng, "Do environmental markets cause environmental injustice? Evidence from California's carbon market," *Journal of Public Economics*, 2023, *217*, 104786.

Imperial Irrigation District, "Imperial Irrigation District Annual Water QSA Implementation Report," Technical Report 2021.

Johnston, Jill E, Mitiasoa Razafy, Humberto Lugo, Luis Olmedo, and Shohreh F Farzan, "The disappearing Salton Sea: A critical reflection on the emerging environmental threat of disappearing saline lakes and potential impacts on children's health," *Science of the Total Environment*, 2019, *663*, 804–817.

Jones, Benjamin A., "After the Dust Settles: The Infant Health Impacts of Dust Storms," *Journal of the Association of Environmental and Resource Economists*, 2020, *7* (6), 1005–1032.

_ **and John Fleck**, "Shrinking Lakes, Air Pollution, and Human Health: Evidence from California's Salton Sea," *Science of the Total Environment*, 2020, *712*, 136490.

Jones, Benjamin, Jingjing Wang, and John Fleck, "Sending Agricultural Water to The Salton Sea to Improve Public Health? An Integrated Hydro-Agri-Health Economic Analysis," *An Integrated Hydro-Agri-Health Economic Analysis*, 2022.

King, James, Vic Etyemezian, Mark Sweeney, Brenda J Buck, and George Nikolich, "Dust emission variability at the Salton Sea, California, USA," *Aeolian Research*, 2011, *3* (1), 67–79.

Kittle, Sarah, "Survey of reported health effects of Owens lake particulate matter," *Great Basin Unified Air Pollution Control District*, 2000.

_ , "Survey of Reported Health Effects of Owens Lake Particulate Matter," 2000. Great Basin Unified Air Pollution Control District, Bishop, CA.

Kramer, Amber L, Jonathan Liu, Liqiao Li, Rachel Connolly, Michele Barbato, and Yifang Zhu, "Environmental justice analysis of wildfire-related PM2. 5 exposure using low-cost sensors in California," *Science of The Total Environment*, 2023, *856*, 159218.

Libecap, Gary D, *Contracting for property rights*, Cambridge university press, 1993.

Lipsett, M, S Smorodinsky, P English, and L Copan, "Basta border asthma & allergies study: Final report," *Impact Assessment, Inc.: Richmond, VA, USA*, 2009, p. 81.

MacDougall, C.R. and M.F. Uhl, "Empirical Method of Determining Fugitive Dust Emissions from Wind Erosion of Vacant Land: "The MacDougall Method".," Technical Report, Memorandum prepared from the Clark County Department of Air Quality Management, Las Vegas, NV. URL: https://www3.epa.gov/ttn/chief/conference/ei12/fugdust/macdougall.pdf 2002.

Messager, Mathis Loïc, Bernhard Lehner, Günther Grill, Irena Nedeva, and Oliver Schmitt, "Estimating the volume and age of water stored in global lakes using a geo-statistical approach," *Nature communications*, 2016, *7* (1), 13603.

Miao, Yaning, William C Porter, Kurt Schwabe, and Jenna LeComte-Hinely, "Evaluating health outcome metrics and their connections to air pollution and vulnerability in Southern California's Coachella Valley," *Science of the Total Environment*, 2022, *821*, 153255.

Pelt, R Scott Van, John Tatarko, Thomas E Gill, Chunping Chang, Junran Li, Iyasu G Eibedingil, and Marcos Mendez, "Dust emission source characterization for visibility hazard assessment on Lordsburg Playa in Southwestern New Mexico, USA," *Geoenvironmental Disasters*, 2020, *7*, 1–12.

Rahn, David A and Christopher J Mitchell, "Diurnal climatology of the boundary layer in Southern California using AMDAR temperature and wind profiles," *Journal of Applied Meteorology and Climatology*, 2016, *55* (5), 1123–1137.

Tessum, Christopher W, Joshua S Apte, Andrew L Goodkind, Nicholas Z Muller, Kimberley A Mullins, David A Paolella, Stephen Polasky, Nathaniel P Springer, Sumil K Thakrar, Julian D Marshall et al., "Inequity in consumption of goods and services adds to racial–ethnic

disparities in air pollution exposure," *Proceedings of the National Academy of Sciences*, 2019, *116* (13), 6001–6006.

Udall, Bradley and Jonathan Overpeck, "The twenty-first century Colorado River hot drought and implications for the future," *Water Resources Research*, 2017, *53* (3), 2404–2418.

Wurtsbaugh, Wayne A, Craig Miller, Sarah E Null, R Justin DeRose, Peter Wilcock, Maura Hahnenberger, Frank Howe, and Johnnie Moore, "Decline of the world's saline lakes," *Nature Geoscience*, 2017, *10* (11), 816–821.

7 Appendix

Figure A1: Example Particle Trajectories

Notes: This figure demonstrates example particle trajectories from one point on the Salton Sea playa. The point is in black and the red lines indicate particle trajectories that begin at the black playa grid cell.

Figure A2: Location of monitors in the study sample

Panel a) PM_{10} monitors

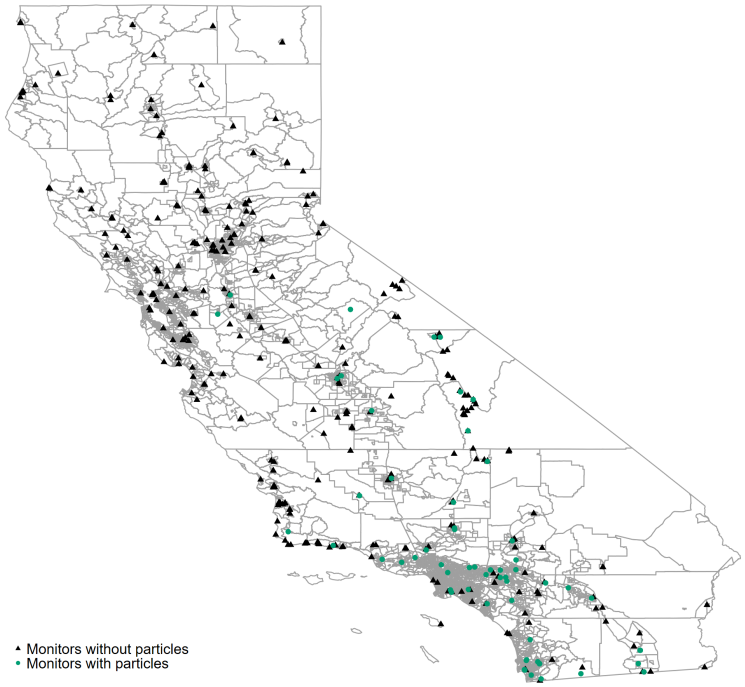

Panel b) $PM_{2.5}$ monitors

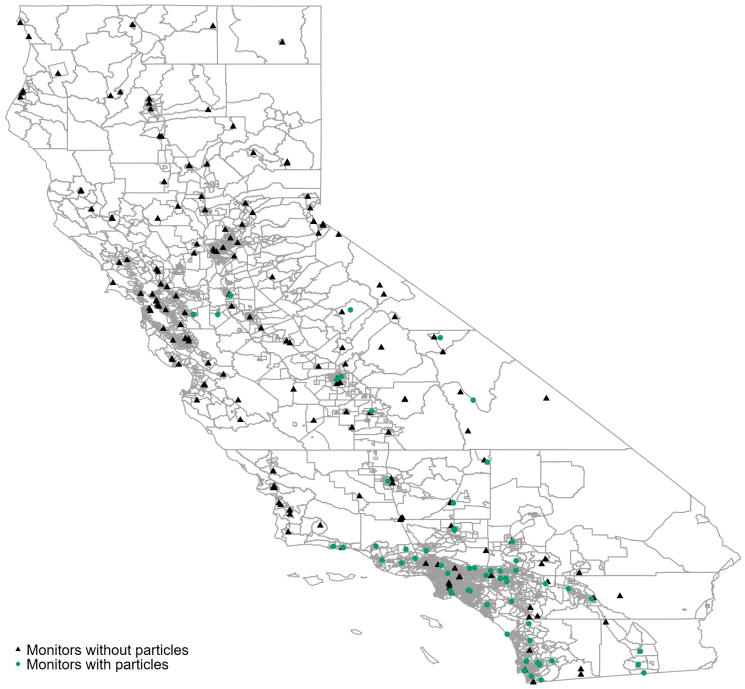

Notes: This figure presents the monitors in the final sample, the green circles represent monitors with particles and the black triangles represent monitors without particles recorded in the buffer of the monitor.

Figure A3: Total Particles by Exposed Playa

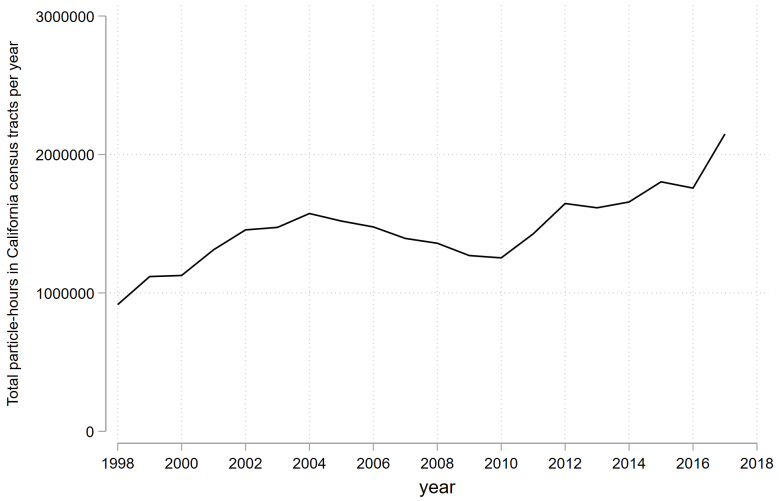

Notes: This figure presents the total number of particle hours in California census tracts over time. Increases in particle hours come from both increasing the amount of source pollution (as more playa is exposed) and from meteorological conditions that lead to particles spending more time in CA census tracts. Particles restricted to a boundary layer of 1,000m.

Figure A4: Exposure to Particle-Hours by Socioeconomic Indicators

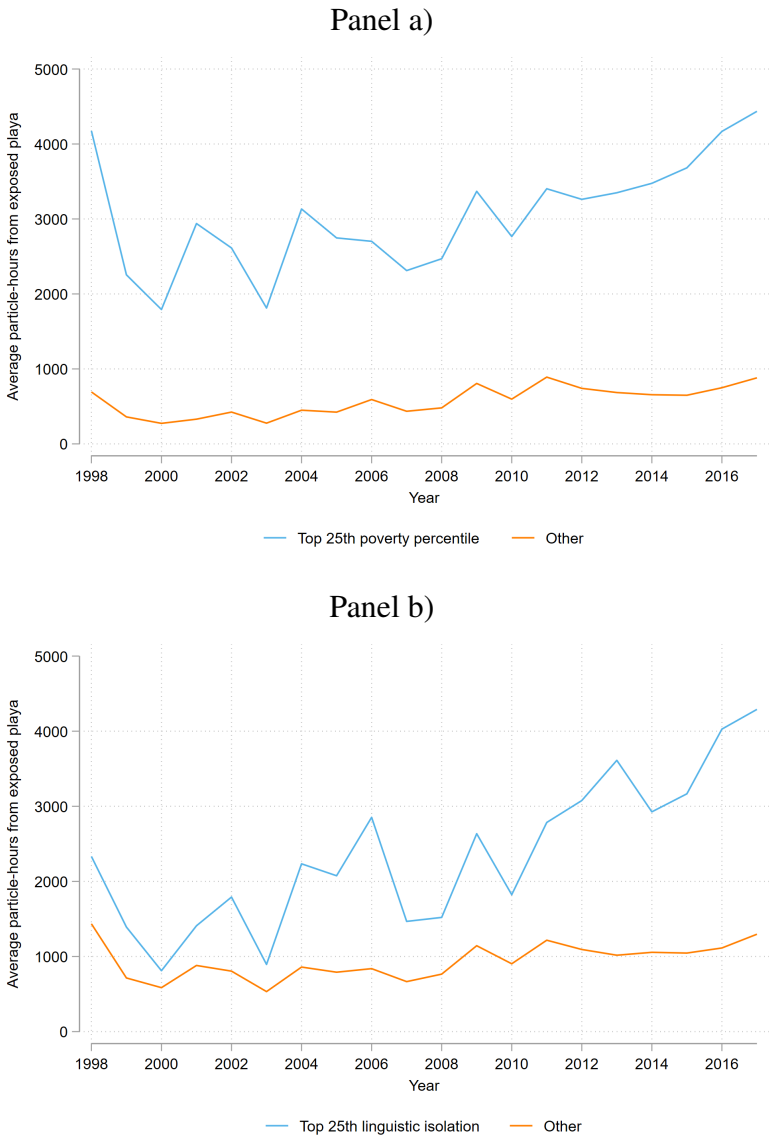

Notes: This figure presents the average particle-hours exposure for the period 1998-2017. For two different indicators: poverty (Panel a) and linguistic isolation (Panel b) in California. Panel a shows average particle-hour exposure for the top 25th poverty percentile (blue) and remaining communities (orange). Panel b shows average particle-hour exposure for top 25th linguistic isolation percentile (blue) and remaining communities (orange). Particle-hour exposure was modeled using HYSPLIT. Particles restricted to a boundary layer of 1,000 meters. Percent poverty and linguistic isolation indicators were obtained from CES4.0.

Table A1: Exposed Playa and Pollution Outcomes -Particles within 500m

	(1) PM_{10}	(2) PM_{10}	(3) PM_{10}	(4) $PM_{2.5}$	(5) $PM_{2.5}$	(6) $PM_{2.5}$
Total particles	1.303***	1.405***	1.439***	0.823***	0.771***	0.769***
	(0.332)	(0.290)	(0.293)	(0.202)	(0.202)	(0.203)
Mean	43.288	43.288	43.288	10.747	10.747	10.747
Obs.	258,640	258,640	258,640	226,548	226,548	226,548
R-squared	0.112	0.139	0.153	0.259	0.288	0.292
Year FE	Yes	Yes	Yes	Yes	Yes	Yes
Month FE	No	Yes	Yes	No	Yes	Yes
Site by point FE	Yes	Yes	Yes	Yes	Yes	Yes
Day of week FE	No	No	Yes	No	No	Yes
Cluster level	Site	Site	Site	Site	Site	Site

Notes: Above are coefficient estimates of β from Equation (1). Columns (1) through (3) use PM_{10} concentrations and Columns (4) through (6) use $PM_{2.5}$ as outcome variables. Fixed effects are indicated by column labels and all standard errors are clustered at the monitor level. The mean indicates the average pollution concentration for the respective pollutant. Particles restricted to have a maximum height of 500 meters.

Table A2: Exposed Playa and Pollution Outcomes with weather controls

	(1) PM_{10}	(2) PM_{10}	(3) PM_{10}	(4) $PM_{2.5}$	(5) $PM_{2.5}$	(6) $PM_{2.5}$
Total particles	1.264***	1.138***	1.188***	0.412***	0.364***	0.368***
	(0.105)	(0.111)	(0.120)	(0.065)	(0.071)	(0.073)
Mean	43.222	43.222	43.222	10.785	10.785	10.785
Obs.	265,093	265,093	265,093	231,768	231,768	231,768
R-squared	0.152	0.163	0.176	0.325	0.351	0.353
Year FE	Yes	Yes	Yes	Yes	Yes	Yes
Month FE	No	Yes	Yes	No	Yes	Yes
Site by point FE	Yes	Yes	Yes	Yes	Yes	Yes
Day of week FE	No	No	Yes	No	No	Yes
Cluster level	Site	Site	Site	Site	Site	Site

Notes: Above are coefficient estimates of β from Equation (1). Columns (1) through (3) use PM_{10} concentrations and Columns (4) through (6) use $PM_{2.5}$ as outcome variables. All the columns include the following weather controls: maximum air temperature, total precipitation, wind speed, and specific humidity. Fixed effects are indicated by column labels and all standard errors are clustered at the monitor level. The mean indicates the average pollution concentration for the respective pollutant. Particles restricted to have a maximum height of 1,000 meters.

Table A3: Exposed Playa and Pollution Outcomes in days without rainfall

	(1) PM_{10}	(2) PM_{10}	(3) PM_{10}	(4) $PM_{2.5}$	(5) $PM_{2.5}$	(6) $PM_{2.5}$
Total particles	1.312***	1.392***	1.431***	0.831***	0.777***	0.776***
	(0.347)	(0.303)	(0.308)	(0.205)	(0.208)	(0.210)
Mean	43.669	43.669	43.669	10.886	10.886	10.886
Obs.	255,062	255,062	255,062	221,030	221,030	221,030
R-squared	0.112	0.137	0.152	0.255	0.285	0.289
Year FE	Yes	Yes	Yes	Yes	Yes	Yes
Month FE	No	Yes	Yes	No	Yes	Yes
Site by point FE	Yes	Yes	Yes	Yes	Yes	Yes
Day of week FE	No	No	Yes	No	No	Yes
Cluster level	Site	Site	Site	Site	Site	Site

Notes: Above are coefficient estimates of β from Equation (1) for days without recorded rainfall. Columns (1) through (3) use PM_{10} concentrations and Columns (4) through (6) use $PM_{2.5}$ as outcome variables. Fixed effects are indicated by column labels and all standard errors are clustered at the monitor level. The mean indicates the average pollution concentration for the respective pollutant. Particles restricted to have a maximum height of 1,000 meters.

Table A4: Exposed Playa and Polution Outcomes in days with any rainfall interactions

	(1) PM_{10}	(2) PM_{10}	(3) PM_{10}	(4) $PM_{2.5}$	(5) $PM_{2.5}$	(6) $PM_{2.5}$
Total particles	1.279***	1.374***	1.412***	0.821***	0.770***	0.769***
	(0.336)	(0.295)	(0.299)	(0.202)	(0.204)	(0.205)
Total particles$\times$ 1{any rain}	-1.512**	-1.476**	-1.682**	-0.247***	-0.291**	-0.298**
	(0.573)	(0.684)	(0.758)	(0.086)	(0.119)	(0.137)
1{any rain}	-10.012***	-8.680***	-9.360***	-2.088***	-2.349***	-2.300***
	(1.864)	(1.972)	(2.227)	(0.243)	(0.328)	(0.324)
Mean	43.222	43.222	43.222	10.785	10.785	10.785
Obs.	265,093	265,093	265,093	231,768	231,768	231,768
R-squared	0.117	0.143	0.157	0.260	0.289	0.293
Year FE	Yes	Yes	Yes	Yes	Yes	Yes
Month FE	No	Yes	Yes	No	Yes	Yes
Site by point FE	Yes	Yes	Yes	Yes	Yes	Yes
Day of week FE	No	No	Yes	No	No	Yes
Cluster level	Site	Site	Site	Site	Site	Site

Notes: Above are coefficient estimates of β from Equation (1) and an interaction with an indicator variable if any rain occurred that day. Columns (1) through (3) use PM_{10} concentrations and Columns (4) through (6) use $PM_{2.5}$ as outcome variables. Fixed effects are indicated by column labels and all standard errors are clustered at the monitor level. The mean indicates the average pollution concentration for the respective pollutant. Particles restricted to have a maximum height of 1,000 meters.

Table A5: Exposed Playa and Polution Outcomes by distance from the Salton Sea

Panel a) Monitors within 100 miles from the Salton Sea

	(1) PM_{10}	(2) PM_{10}	(3) PM_{10}	(4) $PM_{2.5}$	(5) $PM_{2.5}$	(6) $PM_{2.5}$
Total particles	1.269***	1.370***	1.405***	0.818***	0.766***	0.765***
	(0.326)	(0.282)	(0.284)	(0.200)	(0.200)	(0.200)
Mean	43.239	43.239	43.239	10.781	10.781	10.781
Obs.	264,815	264,815	264,815	231,010	231,010	231,010
R-squared	0.112	0.139	0.152	0.256	0.285	0.289
Year FE	Yes	Yes	Yes	Yes	Yes	Yes
Month FE	No	Yes	Yes	No	Yes	Yes
Site by point FE	Yes	Yes	Yes	Yes	Yes	Yes
Day of week FE	No	No	Yes	No	No	Yes
Cluster level	Site	Site	Site	Site	Site	Site

Panel b) Monitors farther than 100 miles from the Salton Sea

	(1) PM_{10}	(2) PM_{10}	(3) PM_{10}	(4) $PM_{2.5}$	(5) $PM_{2.5}$	(6) $PM_{2.5}$
Total particles	-1.322	0.906	0.704	1.208	-0.651	-0.547
	(1.362)	(0.741)	(0.566)	(1.331)	(0.704)	(0.674)
Mean	26.657	26.657	26.657	11.960	11.960	11.960
Obs.	277	277	277	758	758	758
R-squared	0.808	0.958	0.978	0.625	0.887	0.920
Year FE	Yes	Yes	Yes	Yes	Yes	Yes
Month FE	No	Yes	Yes	No	Yes	Yes
Site by point FE	Yes	Yes	Yes	Yes	Yes	Yes
Day of week FE	No	No	Yes	No	No	Yes
Cluster level	Site	Site	Site	Site	Site	Site

Notes: Above are coefficient estimates of β from Equation (1). Panel a) restricts the sample to monitors within 100 miles from the Salton Sea. Panel b) restricts the sample to monitors farther than 100 miles from the Salton Sea. Columns (1) through (3) use PM_{10} concentrations and Columns (4) through (6) use $PM_{2.5}$ as outcome variables. Fixed effects are indicated by column labels and all standard errors are clustered at the monitor level. The mean indicates the average pollution concentration for the respective pollutant. Particles restricted to have a maximum height of 1,000 meters.

Table A6: Trend-Break Model -Particles within 500m

	(1) All	(2) DAC	(3) Other	(4) All	(5) DAC	(6) Other
Trend × post 2011	0.032	0.075***	0.017	0.071**	0.130***	0.051
	(0.02090)	(0.02158)	(0.02718)	(0.03555)	(0.03139)	(0.04290)
Post 2011	-0.053	-0.025	-0.059	0.103***	0.201***	0.076***
	(0.06201)	(0.06575)	(0.06481)	(0.01465)	(0.02072)	(0.01734)
Trend	0.019	0.014	0.020	-0.020	-0.041	-0.014
	(0.02194)	(0.02842)	(0.02143)	(0.03638)	(0.04117)	(0.03694)
Mean	36.327	36.057	36.414	40.860	42.192	40.442
Obs.	767,760	188,160	579,600	542,880	129,420	413,460
Census tract FE	Yes	Yes	Yes	Yes	Yes	Yes
Cluster level	County	County	County	County	County	County
Period	1998-2017	1998-2017	1998-2017	2003-2017	2003-2017	2003-2017

Notes: This table shows the results for equation (2) separately for All (columns 1 and 4), Disadvantaged (columns 2 and 5) and non-Disadvantaged (columns 3 and 6) communities. Columns 1-3 show the results for the entire study period and Columns 4-6 show the results for the 2003-2017 period. Results restricted to particles below 500 m height from ground level. Disadvantaged communities classification was obtained from CES4.0.